

Diverse histomorphology of HER2 positive breast carcinomas based on differential ER expression

Short title: Histomorphology of HER2-positive breast cancer

Momoko Akashi^{1,2}, Rin Yamaguchi^{1,3,*}, Hironori Kusano¹, Hitoshi Obara⁴, Miki Yamaguchi⁵, Uhi Toh², Jun Akiba⁶, Tatsuyuki Kakuma⁴, Maki Tanaka⁵, Yoshito Akagi², Hirohisa Yano¹

¹Department of Pathology, Kurume University School of Medicine, Kurume, Fukuoka, Japan

²Department of Surgery, Kurume University School of Medicine, Kurume, Fukuoka, Japan

³Department of Pathology and Laboratory Medicine, Kurume University Medical Centre, Kurume, Fukuoka, Japan

⁴Biostatistics Centre, Kurume University School of Medicine, Kurume, Fukuoka, Japan

⁵Department of Surgery, Japan Community Healthcare Organization Kurume General Hospital, Kurume, Fukuoka, Japan

⁶Department of Diagnostic Pathology, Kurume University Hospital, Kurume, Fukuoka, Japan

*Corresponding author: Rin Yamaguchi, Department of Pathology and Laboratory Medicine, Kurume University Medical Centre, 155-1 Kokubu, Kurume, Fukuoka 839-0863, Japan.

Tel: +81 942 22 6111; Fax: +81 942 22 6657; E-mail: rin@med.kurume-u.ac.jp

Conflicts of interest: There are no conflicts of interest to disclose.

Funding: The study was partially supported by JSPS KAKENHI grant number JP17K08707.

ABSTRACT

Aims: HER2-positive (HER2+) breast carcinoma (BC) cases are often treated similarly; however, they can be classified as either luminal B (LH) or non-luminal type (NLH) BC, which have different prognoses. In this study, we investigated the clinicohistomorphological features of each HER2+ BC subgroup.

Methods and results: We classified 166 patients with HER2+ invasive BC into LH (n=110 [66.3%]) and NLH groups (n=56 [33.7%]). We further sub-classified LH into patients with carcinomas expressing high levels of hormone receptors (LH-high; Allred score, oestrogen receptor [ER] and/or progesterone receptor [PgR] 4–8) (n=89 [53.6%]) or low levels (LH-low; Allred score, ER and/or PgR 2 or 3) (n=21 [12.7%]) for clinicohistomorphological characterization. Morphological review showed that NLH included a percentage of patients with comedo necrosis, while LH patients had significantly more central scarring. In terms of immune responsiveness, NLH showed significantly higher rates of tumour-infiltrating lymphocytes and healing. The LH-high and NLH groups showed distinct characteristics (by both models, $P<0.05$) and the LH-low group appeared to demonstrate intermediate characteristics according to multinomial analyses using covariates reflecting tumour morphology and immune response outcomes.

Conclusions: These results support the classification of HER2+ BC into two major subgroups, LH-high and NLH, based on tumour morphology and immune response; LH-high proliferates via scirrhous and/or spiculated growth with a central scar, while the primary proliferation pattern of NLH is based on *in situ* carcinomas containing comedo necrosis with noticeable TILs and healing.

KEYWORDS

HER2-positive breast carcinoma; comedo necrosis; tumour-infiltrating lymphocyte; central scar; oestrogen receptor

INTRODUCTION

Breast carcinomas (BC) can be classified histologically and by molecular subtyping.^{1,2} Clinicopathological definitions are based on individual immunohistochemical (IHC) profiles of oestrogen receptor (ER), progesterone receptor (PgR), HER2, and Ki-67 expression. BC can thus be divided into luminal A, luminal B (HER2⁻), luminal B (HER2⁺), HER2⁺ (non-luminal), and triple-negative (TN) subtypes,³ and personalised therapy is recommended for each subtype.⁴ Recent studies indicated that histological classification and molecular subtypes are closely related.^{5,6} Furthermore, subtype-specific characteristics may be reflected in tumour images, suggesting a relationship between subtype and tumour morphology.^{7,8}

HER2⁺ BC is defined as BC with HER2 gene amplification or protein overexpression. Its prognosis has traditionally been poor,⁹ but has improved following good responses to anti-HER2 therapy.¹⁰ Histologically, HER2⁺ BC displays a high degree of atypia,¹¹ no tubular structures,¹² and apocrine differentiation.¹³ Morphologically, HER2⁺ BC and TN BC are similar, with a high percentage of oval or round tumours with microlobulated margins, while luminal types exhibit spiculated (stellate) shapes.⁷ Furthermore, BCs with a large area of comedo necrosis within the ducts are more likely to be HER2⁺,^{14,15} suggesting an association with pleomorphic

linear (or casting type) calcification on diagnostic images. Invasive BC with casting type calcification, of which most cases are malignant,¹⁶ has a poor prognosis compared with other calcifications, and early detection may be important for screening.¹⁷

As noted, HER2+ BC can be divided clinicopathologically into luminal B or non-luminal subtypes,³ though these are typically grouped together for anti-HER2 therapy. However, HER2+ BC can be further subclassified by genotyping, and hormone receptor expression levels can influence HER2+ BC treatment response.^{18,19} Histological features and tumour microenvironment differ between hormone-positive and -negative HER2+ BCs, and indicate different prognoses.²⁰ Thus, HER2+ BC is clinicopathologically heterogeneous, and differences may relate to tumour morphology, although there are few reports.

We classified HER2+ BC into subgroups and investigated their respective clinicopathological characteristics, focusing on morphological appearance associated with comedo or comedo-like necrosis and central scarring.

MATERIALS AND METHODS

Subjects

The study cohort comprised patients with HER2+-invasive BC undergoing surgery but

not neoadjuvant chemotherapy at the Japan Community Health Care Organization Kurume General Hospital between 2013 and 2016. Resected tissue specimens were paraffin-embedded, processed routinely, cut at 4 μm , and stained with haematoxylin and eosin. Immunostaining was performed using biopsy specimens, and for cases in which biopsy specimens could not be used, immunostaining was performed on resected specimens. All slides were reviewed by two pathologists (MA and RY). This retrospective study was approved by the Kurume General Hospital Ethical Committee (No. 187) and Kurume University Ethical Committee (No. 16272).

Immunohistochemistry

ER, PgR, and HER2 were detected by IHC using BenchMark XT (Ventana, Tucson, AZ, USA) according to the manufacturer's protocols. Primary antibodies were ER (clone SP1), PgR (clone IE2), and HER2 (C-erbB-2; clone 4B5) (all Ventana). ER and PgR expression were scored using the Allred score (0–8), calculated from the proportion of positive tumour cells and intensity of immunoreactivity.²¹ A score ≥ 2 was considered positive, 2–3 as low, and ≥ 4 as high expression. Tumours with ER or PgR ≥ 4 were classified as luminal HER2 (LH)-high, those with both ER and PgR scores ≤ 3 as LH-low, and tumours with both ER and PgR scores of 0 as HER2+ (non-luminal) type

(NLH). HER2 IHC expression was assessed according to ASCO/CAP guidelines 2013.²² Specimens with an IHC score 2+ were retested by HER2 dual-colour *in situ* hybridization (DISH), and cases with a HER2/CEP17 rate >2.0 or HER2 copy number >6.0 were determined as positive. We repeated IHC on all outside cases that had been judged as HER2-positive, then performed ISH on all cases with an IHC score ≤ 2 .

Clinicopathologic factors

Clinical information was extracted from pathological records. Subjects were classified as LH or NLH based on ER/PgR/HER2 expression.³ LH patients were further subclassified as LH-high or LH-low. Comedo/comedo-like necrosis, *in situ* carcinoma, micro/minimal invasion, apocrine features, healing, central scarring with or without elastosis, medullary, invasive micropapillary, squamous, and pleomorphic lobular features, tumour-infiltrating lymphocytes (TILs), histological grade, and macroscopic/magnifying classification were examined for each group.

Definitions of histological features

Histological grade was classified as 1–3.²³ Carcinomas in which the carcinoma cells proliferated *in situ* were defined as *in situ* carcinomas, and any degree of necrotic

material surrounded by viable carcinoma cells in the duct or ductal-based proliferation in invasive foci was regarded as comedo or comedo-like necrosis.²⁴ TILs were defined as lymphocytes infiltrating the tumour stroma,²⁵ and were considered positive if they occurred in $\geq 50\%$ of the stroma. Cases with eosinophilic granular cytoplasm, indicating apocrine metaplasia, in $\geq 10\%$ of the tumour were regarded as apocrine features.¹³ Healing was defined as thick fibrosis or phagocytosis surrounding an *in situ* or *in situ*-based carcinoma, including some phases with or without TILs (Fig. 1A–C).^{14, 15, 26,}

²⁷ Tumours with high-grade nuclear atypia, a syncytial growth pattern, marked lymphocytic infiltration, and rounded borders were considered as presenting medullary features,²⁸ while those in which $\geq 10\%$ of carcinoma cells formed micropapillary structures were regarded as showing invasive micropapillary features, $\geq 5\%$ of carcinoma cells with squamous metaplasia as squamous features, invasive area ≤ 1 mm as microinvasion, and an invasive area ≤ 5 mm as minimal invasion. To evaluate the central scar, we used image analysis. Tumour maximum cross-section slide images were obtained using the NanoZoomer (Hamamatsu Photonics, Hamamatsu, Japan), then whole tumours and central scarring areas were measured using NDP view2 (Hamamatsu Photonics, Hamamatsu, Japan). Tumours in which $\geq 10\%$ of the whole area of fibrosis (scarring) consisted of fibroblasts and collagenous fibres were regarded as having a

central scar (Fig. 2). Any degree of elastic changes identified in central scarring was regarded as elastosis.

Scoring

Comedo necrosis and *in situ* carcinoma were scored according to the mean proportion of each lesion's area in three visual fields (approximately 11.5 mm²/field) randomly selected from the tumour's maximum cross-section: comedo necrosis score 1= \leq 1%; 2=1%– $<$ 10%; 3= \geq 10%; *in situ* carcinoma score 1= \leq 15%; 2=15%– $<$ 30%; 3= \geq 30% (Fig. 3 and 4). Lesion areas were measured using the Nanozoomer and NDP.view2. When a lesion was small and three fields of vision could not be assessed, it was measured in one or two fields of vision. TIL percentages were measured according to TILs Working Group 2014 criteria,²⁵ and scored: TIL score 1= \leq 33%; 2=33%– $<$ 66%; and 3= \geq 66% (Fig. 5A–C).

Macroscopic/magnifying classification

Tumour macroscopic/magnifying classification was classified as a1, a2, or a3, according to morphological features.²⁹ Type a1 was defined as predominantly *in situ* proliferation (Fig. 6A), type a2 as solid/ring-like growth pattern (Fig. 6B), and type a3 as spiculated

growth pattern with a strong tendency to invade the surrounding tissues (Fig. 6C).²⁹ If multiple macroscopic types were present, the tumour was classified according to the type occupying the largest area.

Morphological and immune response models

Univariate multinomial logistic regression was applied to assess relationships between the histomorphological features and tumour morphology and immune response in each group. Comedo necrosis (score 1–3) and central scarring (present or absent) were extracted in the tumour morphology model, and healing (present or absent), TIL (score 1–3), and comedo necrosis (score 1–3) in the immune response model.

Histomorphological features in each group were examined simultaneously using the classification and regression tree (CART) model.³⁰ Asymmetric combinations of histomorphological features were examined in both models. Multinomial logistic regression was then used to test the effects of the asymmetric histomorphological features in each group. The probability of membership of each group was calculated to characterize the morphological and immune response patterns.

Statistical analysis

Multinomial logistic regression models were used to analyse each group using STATA 15. CART³⁰ was fitted to construct clinicohistomorphological profiles for each group using Jump Pro 13. Pearson's χ^2 or Fisher's exact tests were performed as required. Prognosis was evaluated by disease-free survival (DFS), defined as the number of days between the date of first diagnosis of invasive BC and the date of metastatic recurrence or last follow-up. DFS was estimated using the Kaplan–Meier method, and differences in DFS between subgroups were compared by log-rank test.

$P \leq 0.05$ was considered statistically significant. Multiplicity was adjusted by the Bonferroni method.

RESULTS

Clinicopathological characteristics

A total of 1301 cases of invasive BC surgery were performed between 2013 and 2016, of which 218 were HER2+ (16.8%). Among these, 49 patients who underwent neoadjuvant chemotherapy and three who were previously diagnosed as IHC HER2 score 3+ but rejudged as HER2– by DISH or fluorescence *in situ* hybridization were excluded. All patients were female (median age, 59 years). There were 110 patients in the LH group (66.3%) (LH-high 89 [53.6%], LH-low 21 [12.7%]) and 56 (33.7%) in the

NLH group. Twelve cases of Allred score 4 and 5 were LH-high, and only one case had an intensity score of 1 (weak intensity); all other cases had intensity scores of ≥ 2 . Table 1 details the clinicopathological characteristics of each group.

Histological features

Table 1 presents the relationships between histological features and HER2-positive BC. All three subgroups included numerous histological grade 3 cases, with no significant difference among subgroups. The incidences of comedo/comedo-like necrosis, micro/minimal invasion, TILs, apocrine features, healing, medullary features, and squamous features were all significantly higher in LH-low or NLH compared with LH-high, while central scarring was significantly more common in LH-high than NLH. Although half of the central scars presented with elastosis, there were no significant differences in elastosis among the three groups with central scars. There were no significant differences in terms of *in situ* carcinoma and other features.

Scoring

Scores are shown in Table 2. Significantly more patients in the NLH group had a score of 3 for all three factors (comedo necrosis, *in situ* carcinoma, TILs) compared with the

LH-high group.

Macroscopic/magnifying classifications

Macroscopic/magnifying classifications in each group are shown in Table 3. The incidence of spiculated-growth type (a3) was significantly higher in the LH-high group, and the incidence of *in situ*-predominant proliferation (a1) was significantly higher in the NLH group.

Morphological and immune response models

The morphological and immune response models including CART models are shown in Figure 7 and 8. LH-high and NLH showed different trends in both models, and significant differences were confirmed by likelihood-ratio tests (morphological and immune response models, both $P < 0.05$). The LH-low group appeared to demonstrate intermediate characteristics, but the result was not significant because of the small number of cases.

Prognosis

There was only one death in the NLH group and 10 cases (LH-high, 4; LH-low, 0; NLH,

6) of metastatic recurrence during follow-up (median, 972.5 days). There was no significant difference in DFS among the three subgroups, but DFS was significantly lower in the NLH group ($P=0.04$) compared with the LH group (log-rank test).

DISCUSSION

We defined clinicohistomorphological features of HER2+ BC by univariate analyses, and extracted four groups using the CART model. Multinomial logistic regression was then used to examine relationships between the four groups with the three BC groups. Consistent with reports describing HER2+ BC as a high-grade carcinoma,¹¹ the present results showed no intergroup differences in histological grade, and high-grade nuclear atypia appeared to be a homogenous feature of HER2+ BC subgroups. Comedo/comedo-like necrosis was not robust in the active surveillance of low-risk DCIS.³¹ Therefore, we described any necrotic debris as comedo or comedo-like necrosis within the duct or *in situ*-based invasive proliferation in the present study. This was observed in 77.1% of patients across all HER2+ BC types. In particular, the comedo necrosis and *in situ* lesion scores were significantly higher ($P<0.001$) in NLH than LH-high. These results suggested that, although comedo necrosis occurred in some LH-high patients, *in situ* or *in situ* carcinoma-based proliferation involving comedo

necrosis formed a large part of the morphology in the NLH group. Microinvasive and minimal invasion (≤ 5 mm) are considered the first step in the invasion of *in situ* carcinomas and were significantly more frequent in the NLH group compared with the LH-high group, confirming that the proliferation pattern of HER2+ BC, could be mostly established from intraductal lesions. Therefore, early detection of microinvasive and minimal invasive HER2 BCs could lead to blocking most invasive NLH (>5 mm). Also, we previously described that healing via severe infiltration of CD8+ lymphocytes often occurs in *in situ* and microinvasion of HER2+ BC,¹⁵ and high-TILs were also significantly more frequent in NLH compared with LH-high in the current study, characterized by healing with severe lymphocyte infiltration and medullary features. These results suggest that NLH BCs may represent an immunologically higher responsive group than LH-high. Previous and present studies indicated that NLH showed worse prognosis (DFS) than LH.¹⁰ NLH may be targets for immune checkpoint inhibitors in addition to anti-HER2 therapy.

Macroscopic/magnifying classification also demonstrated a significant association between NLH BC and *in situ*-predominant proliferation type (a1), which may reflect the histological observation that intraductal lesions represented the primary component of NLH tumours. Previously, comedo necrosis was observed as crushed stone-like

lesions,³² and central necrosis with DCIS was observed as casting-type calcification on mammograms,¹⁶ suggesting that HER2+ BC in this study might present with significantly more calcification according to the Breast Imaging Reporting and Data System³³ Category 4 or higher on mammograms, especially in the NLH group.³⁴ While central scarring is sometimes called fibrotic focus (FF), it has been reported to be significantly more common in luminal A than luminal B type and HER2-overexpressing carcinomas.³⁵ FF was sometimes confused with the central acellular zone. To avoid this, we defined central scarring as the formation of fibrosis by collagen materials occupying more than ten percent of the tumour with or without elastosis. Comparisons among the HER2+ BC groups showed a significant correlation between LH-high and central scarring ($P=0.001$). LH-high showed spiculated growth (a3) patterns, frequently detected in tumours with spiculated or partially micro-serrated margins by mammography, indicating that LH-high patients developed similar tumour shapes to luminal types. Tumour phenotypes and proliferation patterns differed by subgroup among patients with HER2+ BC, and these histomorphological features and differences are reflected in diagnostic imaging. Especially, features in *in situ*-based comedo/comedo-like-necroses reflected casting type calcifications¹⁶ that may lead to early detection of NLH groups that have worse prognoses than LH.¹⁰

A recent study of HER2+ BC treatment response and other variables reported heterogeneity,³⁶ and the different histological features and tumour phenotypes observed in the current study may also be associated with different treatment responses. However, the present study had some limitations, including the use of data from a single institution, retrospective observations, the small number of cases, and a relatively short observation period. Nevertheless, our data were relatively robust because the study was performed using consistent processes and all diagnoses were made by the same pathologist throughout the study. We will extend the observation period and perform further future investigations of relationships with imaging findings.

In summary, we identified two major BC classifications, LH-high and NLH, according to tumour morphology and immunological response. LH-high proliferates via scirrhous and/or spiculated growth with a central scar and shows a weaker immunological response than other HER2+ BCs, with less noticeable TILs and healing, while the primary proliferation pattern of NLH is based on *in situ* carcinomas containing comedo necrosis, with a more active immunological response with noticeable TILs and healing. Although LH-low had characteristics intermediate between LH-high and NLH, both the morphological and immune response models seem to suggest that LH-low may be closer to NLH in terms of the nature of the carcinoma. The

results of this study support further research of treatment responses and the prognostic value, which may help to determine treatment options and early detection in patients with HER2+ BC.

ACKNOWLEDGEMENTS

We thank Susan Furness, PhD, and H. Nikki March, PhD, from Edanz Group (www.edanzediting.com/ac) for editing a draft of this manuscript.

AUTHOR CONTRIBUTIONS

R. Yamaguchi is the corresponding author and M. Akashi and RY had a central role in this study. M. Tanaka and M. Yamaguchi are surgeons and provided patient samples. T. Kakuma and H. Obara interpreted the statistical data. U. Toh, J. Akiba and H. Kusano advised on manuscript preparation. H. Yano and Y. Akagi provided administrative support. All authors contributed to the content and approved the final manuscript.

REFERENCES

1. Perou CM, Sorlie T, Eisen MB et al. Molecular portraits of human breast tumours. *Nature* 2000; 406: 747–752.
2. Sorlie T, Perou CM, Tibshirani R et al. Gene expression patterns of breast carcinomas distinguish tumor subclasses with clinical implications. *Proc Natl Acad Sci U S A.* 2001; 98: 10869–10874.
3. Goldhirsch A, Wood WC, Coates AS, et al. Strategies for subtypes dealing with the diversity of breast cancer: highlights of the St. Gallen International Expert Consensus on the Primary Therapy of Early Breast Cancer 2011. *Annals of Oncology* 2011; 22: 1736–1747.
4. Coates AS, Winer EP, Goldhirsch A et al. Tailoring therapies improving the management of early breast cancer: St Gallen International Expert Consensus on the Primary Therapy of Early Breast Cancer 2015. *Annals of Oncology* 2015; 26: 1533–1546.
5. Weigelt B, Geyer FC, Reis-Filho JS. Histological types of breast cancer: how special are they? *Molecular Oncology* 2010; 4: 192–208.
6. Caldarella A, Buzzoni C, Crocetti E et al. Invasive breast cancer: a significant correlation between histological types and molecular subgroups. *Journal of Cancer*

Research and Clinical Oncology 2013; 139: 617–623.

7. Tamaki K, Ishida T, Miyashita M et al. Correlation between mammographic findings and corresponding histopathology: potential predictors for biological characteristics of breast diseases. *Cancer Science* 2011; 102: 2179–2185.

8. Tamaki K, Ishida T, Miyashita M et al. Multidetector row helical computed tomography for invasive ductal carcinoma of the breast: correlation between radiological findings and the corresponding biological characteristics of patients. *Cancer Science* 2012; 103: 67–72.

9. Sorlie T, Tibshirani R, Parker J et al. Repeated observation of breast tumor subtypes in independent gene expression data sets. *Proceedings of the National Academy of Sciences of the United States of America* 2003; 100: 8418–8423.

10. Dawood S, Broglio K, Buzdar AU et al. Prognosis of women with metastatic breast cancer by HER2 status and trastuzumab treatment: an institutional-based review. *Journal of Clinical Oncology* 2010; 28: 92–98.

11. Hoff ER, Tubbs RR, Myles JL et al. HER2/neu amplification in breast cancer: stratification by tumor type and grade. *American Journal of Clinical Pathology* 2002; 117: 916–921.

12. van de Vijver MJ, Peterse JL, Mooi WJ et al. Neu-protein overexpression in

breast cancer. Association with comedo-type ductal carcinoma in situ and limited prognostic value in stage II breast cancer. *The New England Journal of Medicine* 1988; 319: 1239–1245.

13. Bhargava R, Beriwal S, Striebel JM et al. Breast cancer molecular class ERBB2: preponderance of tumors with apocrine differentiation and expression of basal phenotype markers CK5, CK5/6, and EGFR. *AIMM* 2010; 18: 113–118.

14. Morita M, Yamaguchi R, Tanaka M et al. Two progressive pathways of microinvasive carcinoma: low-grade luminal pathway and high-grade HER2 pathway based on high tumour-infiltrating lymphocytes. *Journal of Clinical Pathology* 2016; 69: 890–898.

15. Morita M, Yamaguchi R, Tanaka M et al. CD8(+) tumor-infiltrating lymphocytes contribute to spontaneous "healing" in HER2-positive ductal carcinoma in situ. *Cancer Medicine* 2016; 5: 1607–1618.

16. Tabár L, Tot T, Dean PB. Breast cancer: The art and science of early detection with mammography: Perception, interpretation, histopathologic correlation: Thieme, 2005; viii, 476 p.

17. Tabar L, Tony Chen HH, Amy Yen MF et al. Mammographic tumor features can predict long-term outcomes reliably in women with 1–14-mm invasive breast

carcinoma. *Cancer* 2004; 101; 1745–1759.

18. Llombart-Cussac A, Cortes J, Pare L et al. HER2-enriched subtype as a predictor of pathological complete response following trastuzumab and lapatinib without chemotherapy in early-stage HER2-positive breast cancer (PAMELA): an open-label, single-group, multicentre, phase 2 trial. *The Lancet Oncology* 2017; 18: 545–554.

19. Ellis MJ, Coop A, Singh B et al. Letrozole is more effective neoadjuvant endocrine therapy than tamoxifen for ErbB-1- and/or ErbB-2-positive, estrogen receptor-positive primary breast cancer: evidence from a phase III randomized trial. *Journal of Clinical Oncology* 2001; 19: 3808–3816.

20. Lee HJ, Park IA, Park SY et al. Two histopathologically different diseases: Hormone receptor-positive and hormone receptor-negative tumors in HER2-positive breast cancer. *Breast Cancer Research and Treatment* 2014; 145; 615–623.

21. Allred DC, Harvey JM, Berardo M et al. Prognostic and predictive factors in breast cancer by immunohistochemical analysis. *Modern Pathology* 1998; 11: 155–168.

22. Wolff AC, Hammond ME, Hicks DG et al. Recommendations for human epidermal growth factor receptor 2 testing in breast cancer: American Society of Clinical Oncology/College of American Pathologists clinical practice guideline update.

Journal of Clinical Oncology 2013; 31: 3997–4013.

23. Elston CW, Ellis IO. Pathological prognostic factors in breast cancer. I. The value of histological grade in breast cancer: experience from a large study with long-term follow-up. *Histopathology* 1991; 19: 403–410.

24. Silverstein MJ, Poller DN, Waisman JR et al. Prognostic classification of breast ductal carcinoma-in-situ. *Lancet* 1995; 345: 1154–1157.

25. Salgado R, Denkert C, Demaria S et al. The evaluation of tumor-infiltrating lymphocytes (TILs) in breast cancer: recommendations by an International TILs Working Group 2014. *Annals of Oncology* 2015; 26: 259–271.

26. Muir R, Aitkenhead AC. The healing of intra-duct carcinoma of the mamma. *The Journal of Pathology and Bacteriology* 1934; 38: 117–127.

27. Horii R, Akiyama F, Kasumi F et al. Spontaneous "healing" of breast cancer. *Breast Cancer* 2005; 12: 140–144.

28. Lakhani SR, Ellis IO, Schnitt SJ, Tan PH, van de Vijver MJ eds. WHO Classification of Tumours of the Breast, 4th edn. International Agency for Research on Cancer, 2012.

29. Tsunoda-Shimizu H, Hayashi N, Hamaoka T et al. Determining the morphological features of breast cancer and predicting the effects of neoadjuvant

chemotherapy via diagnostic breast imaging. *Breast Cancer* 2008; 15: 133–140.

30. Zhang H, Singer B. *Recursive Partitioning in the Health Sciences*. New York, NY: Springer-Verlag, 1999.

31. Harrison BT, Hwang ES, Partridge AH, Thompson AM, Schnitt SJ. Variability in diagnostic threshold for comedo necrosis among breast pathologists: Implications for patient eligibility for active surveillance trials of ductal carcinoma in situ. *Modern Pathology : an official journal of the United States and Canadian Academy of Pathology, Inc.* 2019 [Epub ahead of print].

32. Tan PH, Ho JT, Ng EH et al. Pathologic-radiologic correlations in screen-detected ductal carcinoma in situ of the breast: findings of the Singapore breast screening project. *International Journal of Cancer* 2000; 90: 231–236.

33. D’Orsi CJ, Sickles EA, Mendelson EB, Morris EA et al. *ACR BI-RADS® Atlas, Breast Imaging Reporting and Data System*. Reston, VA: American College of Radiology, 2013.

34. Palka I, Ormandi K, Gaal S, Boda K, Kahan Z. Casting-type calcifications on the mammogram suggest a higher probability of early relapse and death among high-risk breast cancer patients. *Acta oncologica (Stockholm, Sweden)* 2007; 46; 1178-1183.

35. Mujtaba SS, Ni YB, Tsang JY et al. Fibrotic focus in breast carcinomas: relationship with prognostic parameters and biomarkers. *Annals of Surgical Oncology* 2013; 20: 2842–2849.
36. Mittendorf EA, Chavez-MacGregor M. All HER2-positive tumors are not created equal. *Annals of Surgical Oncology* 2017; 24: 3471–3474.

Table 1. Clinicopathological characteristics and histological features of HER2+ breast carcinomas

	LH			NLH ^C	Total ^{A+B+C}	P-value	P-value		
	LH-high ^A (n=89)	LH-low ^B (n=21)	Total ^{A+B} (n=110)	(n=56)	(n=166)	(A vs B vs C)	(A vs. B)	(A vs. C)	(B vs C)
Age (years)	57±11.4	62±9.3	59±11.5	59±10.5	59±11.3	0.008*	✓		
Tumour size (cm)	1.6±1.6	1.4±0.9	1.6±1.5	1.3±1.2	1.5±1.4	0.013*		✓	
Histological grade									
1	4 (4.5%)	0 (0%)	4 (3.6%)	1 (1.8%)	5 (3%)	0.112			
2	35 (39.3%)	6 (28.6%)	41 (37.3%)	12 (21.4%)	53 (31.9%)				
3	50 (56.2%)	15 (71.4%)	65 (59.1%)	43 (76.8%)	108 (65.1%)				
Comedo necrosis									
Present	60 (67.4%)	19 (90.5%)	79 (71.8%)	49 (87.5%)	128 (77.1%)	0.006*		✓	
Absent	29 (32.6%)	2 (9.5%)	31 (28.2%)	7 (12.5%)	38 (22.9%)				
<i>In situ</i> carcinoma									
Present	63 (70.8%)	17 (80.6%)	80 (72.7%)	43 (76.8%)	123 (74.1%)	0.54			
Absent	26 (29.2%)	4 (19%)	30 (27.3%)	13 (23.2%)	43 (25.9%)				
Micro/minimal invasion									
Present	0 (0%)	2 (9.5%)	2 (1.8%)	15 (26.8%)	17 (10.2%)	<0.001*	✓	✓	
Absent	89 (100%)	19 (90.5%)	108 (98.2%)	41 (73.2%)	149 (89.8%)				
TIL									
Positive	14 (15.7%)	11 (52.4%)	25 (22.7%)	39 (69.6%)	64 (38.6%)	<0.001*	✓	✓	
Negative	75 (84.3%)	10 (47.6%)	85 (77.3%)	17 (30.4%)	102 (61.4%)				
Apocrine feature									
Present	37 (41.6%)	15 (71.4%)	52 (47.3%)	33 (58.9%)	85 (51.2%)	0.018*	✓		
Absent	52 (58.4%)	6 (28.6%)	58 (52.7%)	23 (41.1%)	81 (48.8%)				
Healing									
Present	16 (18%)	14 (66.7%)	30 (27.3%)	40 (71.4%)	70 (42.2%)	<0.001*	✓	✓	
Absent	73 (82%)	7 (33.3%)	80 (72.7%)	16 (28.6%)	96 (57.8%)				
Central scar									
Present with elastosis	16 (18%)	2 (9.5%)	18 (16.4%)	1 (1.8%)	19 (11.4%)	0.001*		✓	✓
Present without elastosis	15 (16.9%)	3 (14.3%)	18 (16.4%)	1 (1.8%)	19 (11.4%)				
Absent	58 (65.2%)	16 (76.2%)	74 (67.3%)	54 (96.4%)	128 (77.1%)				

Medullary feature								
Present	6 (6.7%)	7 (33.3%)	13 (11.8%)	11 (19.6%)	24 (14.5%)	0.003*	✓	
Absent	83 (93.3%)	14 (66.7%)	97 (88.2%)	45 (80.4%)	142 (85.5%)			
Invasive micropapillary feature								
Present	24 (27%)	6 (28.6%)	30 (27.3%)	6 (10.7%)	36 (21.7%)	0.049*		
Absent	65 (73%)	15 (71.4%)	82 (72.7%)	50 (89.3%)	130 (78.3%)			
Squamous feature								
Present	12 (13.5%)	10 (47.6%)	22 (20%)	19 (33.9%)	41 (24.7%)	<0.001*	✓ ✓	
Absent	77 (86.5%)	11 (52.4%)	88 (80%)	37 (66.1%)	125 (75.3%)			
Pleomorphic lobular feature								
Present	5 (5.6%)	0 (0%)	5 (4.5%)	1 (1.8%)	6 (3.6%)	0.683		
Absent	84 (94.4%)	21 (100%)	105 (95.5%)	55 (98.2%)	160 (96.4%)			

*Indicates significant result. ✓ Bonferroni-adjusted *P*-value (<0.016).

LH, luminal HER2; NLH, non-luminal HER2; TIL, tumour-infiltrating lymphocytes

Table 2. Scoring of HER2+ breast carcinomas

	LH			NLH ^C (n=56)	Total ^{A+B+C} (n=166)	P-value (A vs. B vs. C)	P-value		
	LH-high ^A (n=89)	LH-low ^B (n=21)	Total ^{A+B} (n=110)				(A vs. B)	(A vs. C)	(B vs. C)
Comedo necrosis score									
1	59 (66.3%)	8 (38.1%)	67 (60.9%)	16 (28.6%)	83 (50%)	<0.001*	✓		
2	24 (27%)	11 (52.4%)	35 (31.8%)	21 (37.5%)	56 (33.7%)				
3	6 (6.7%)	2(9.5%)	8 (7.3%)	19 (33.9%)	27 (16.3%)				
<i>In situ</i> lesion score									
1	71 (79.8%)	17 (81%)	88 (80%)	34 (60.7%)	122 (73.5%)	0.04*	✓		
2	11 (12.4%)	1 (4.8%)	12 (10.9%)	8 (14.3%)	20(12%)				
3	7 (7.9%)	3 (14.3%)	10 (9.1%)	14 (25%)	24 (14.5%)				
TIL score									
1	65 (73%)	4 (19%)	69 (62.7%)	16 (28.6%)	85 (51.2%)	<0.001*	✓	✓	
2	19 (21.3%)	8 (38.1%)	27 (24.5%)	17 (30.4%)	44 (26.5%)				
3	5 (5.6%)	9 (42.9%)	14 (12.7%)	23 (41.1%)	37 (22.3%)				

*Indicates significant result. ✓ Bonferroni-adjusted *P*-value (<0.016).

LH, luminal HER2; NLH, non-luminal HER2; TIL, tumour-infiltrating lymphocytes

Table 3. Macroscopic/magnifying classifications of HER2-positive breast carcinomas

	LH			NLH ^C (n=56)	Total ^{A+B+C} (n=166)	P-value (A vs. B vs. C)	P-value	
	LH-high ^A (n=89)	LH-low ^B (n=21)	Total ^{A+B} (n=110)				(A vs. B)	(A vs. C) (B vs. C)
a1	24 (27%)	10 (47.6%)	34 (30.9%)	39 (69.6%)	73 (43.7%)	<0.001*		✓
a2	15 (16.9%)	4(19%)	19 (17.3%)	8 (14.3%)	27 (16.2%)			
a3	50 (56.2%)	7 (33.3%)	57 (51.8%)	9 (16.1%)	66 (39.8%)			

*Indicates significant result. ✓ Bonferroni-adjusted P-value (<0.016).

LH, luminal HER2; NLH, non-luminal HER2; a1, *in situ* predominant proliferation type; a2, solid/ring-like growth type; a3, spiculated growth type.

Figure Legends

Figure 1. Healing. (A) Lymphocyte infiltration with fibrotic changes occurred surrounding high-grade ductal carcinoma in situ. (B) Intraductal fibrosis was observed with background tumour-infiltrating lymphocytes. (C) Near end-stage healing was partially seen in the left area, while invasive carcinoma foci remained in the right area.

Figure 2. Central scarring. Tumour invading the adipose tissue with more than 10% of irregularly shaped fibrotic changes (red line circumscription) composed of fibroblasts and collagen fibres in the centre of the tumour. Elastosis was identified in the central scar.

Figure 3. Scoring of comedo necrosis. The mean proportion of comedo necrosis areas (red line circumscription) in three visual fields (approximately 11.5 mm² per visual field; yellow line circumscription) randomly selected from the tumour's maximum cross-section. Score 1 (<1%), score 2 (1%–<10%), score 3 (≥10%).

Figure 4. Scoring of *in situ* carcinoma. The mean proportion of *in situ* carcinoma areas (blue line circumscription) in three visual fields (approximately 11.5 mm² per visual field; yellow line circumscription) randomly selected from the tumour's maximum cross-section. Score 1 (<15%), score 2 (15%–<30%), score 3 (≥30%).

Figure 5. Scoring of tumour-infiltrating lymphocytes (TILs). Scoring of the proportion

of the stroma surrounding the tumour nests occupied by TILs. (A) Score 1 (<33%), (B) score 2 (34%–66%), and (C) score 3 (\geq 67%).

Figure 6. Macroscopic/magnifying classifications. (A) *In situ*-predominant proliferation type (a1). Small lesions with yellow comedo-like content sporadically intermingled with breast tissue. (B) Solid/ring-like growth type (a2). A solid mass growing expansively in the centre of the tumour. (C) Spiculated growth type (a3). Mass growing radially or irregularly.

Figure 7. CART model (A) and multinomial analysis (B) of HER2-positive breast carcinomas: morphological model. k=1 (central scar present), k=2 (central scar absent and comedo score 1), k=3 (central scar absent and comedo score 2), k=4 (central scar absent and comedo score 3).

Figure 8. CART model (A) and multinomial analysis (B) of HER2-positive breast carcinomas: immune response model. g=1 (healing absent), g=2 (healing present and TIL score \leq 2 and comedo score \leq 2), g=3 (healing present and TIL score \leq 2 and comedo score 3), g=4 (healing present and TIL score 3).

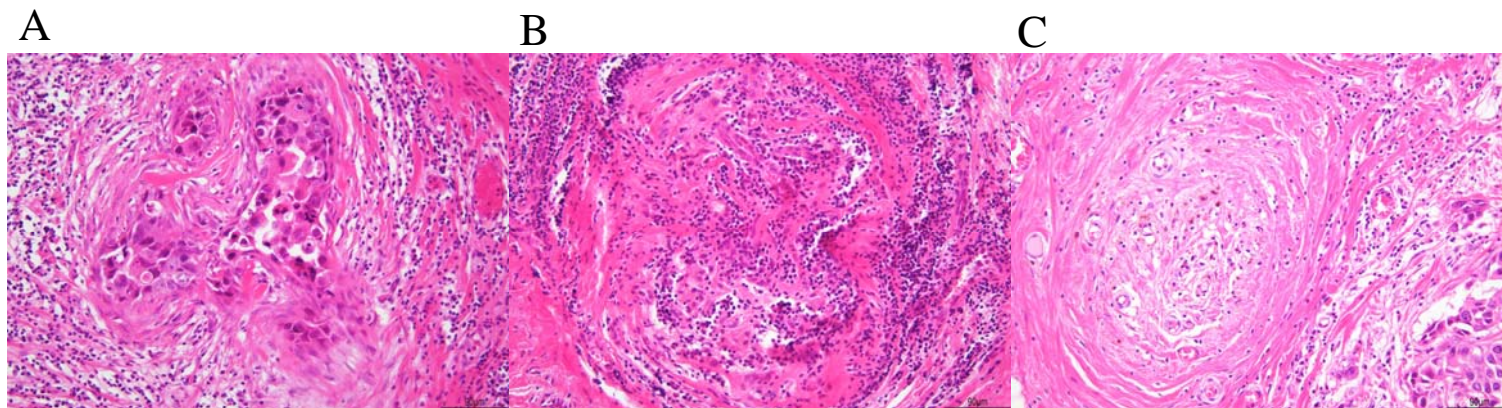


FIGURE 1.

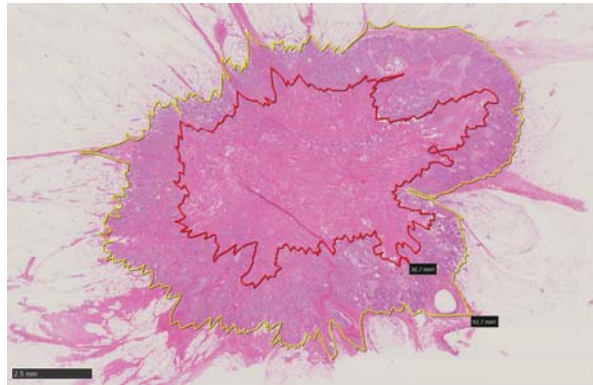


FIGURE 2.

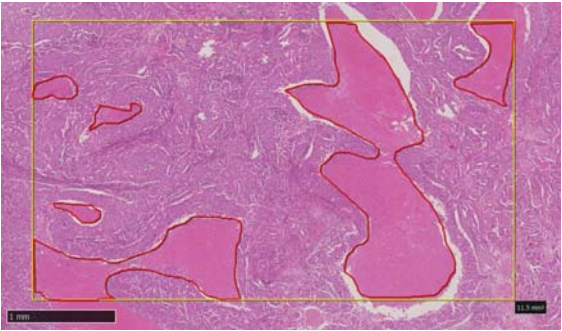


FIGURE 3.

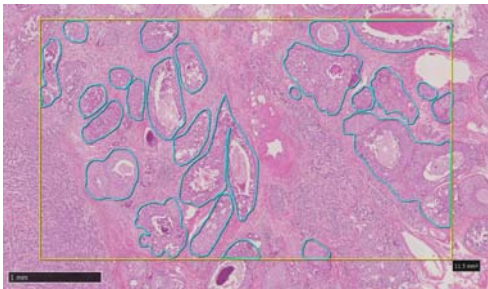


FIGURE 4.

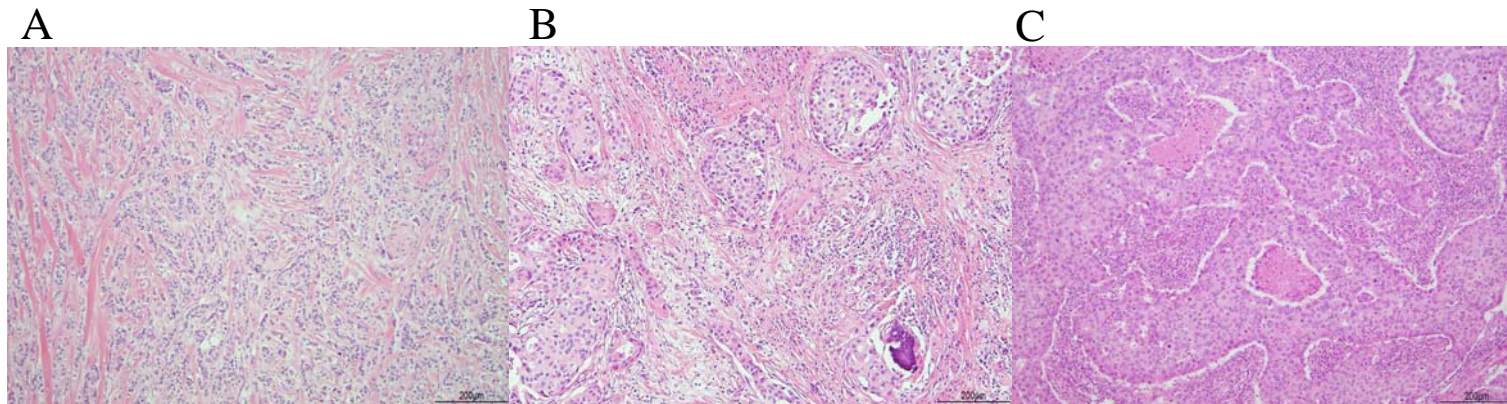


FIGURE 5.

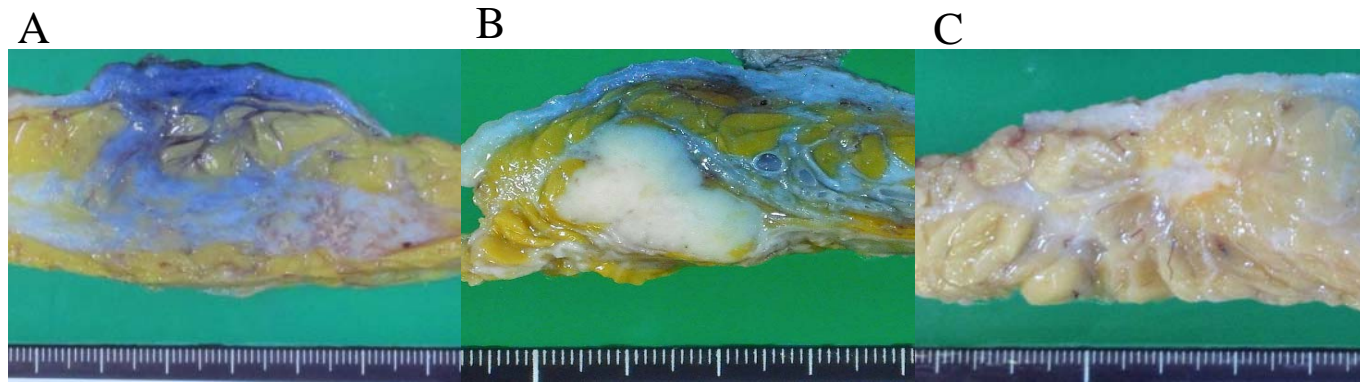


FIGURE 6.

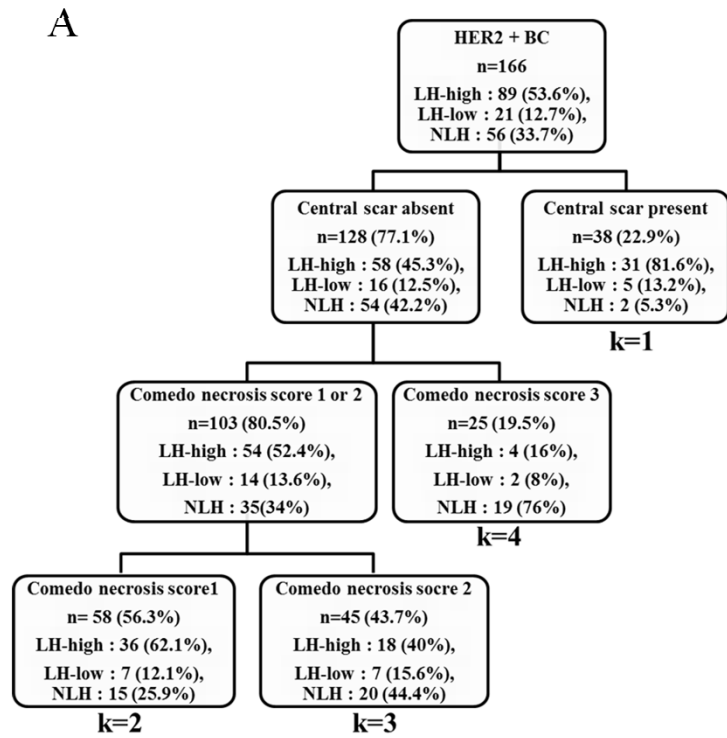
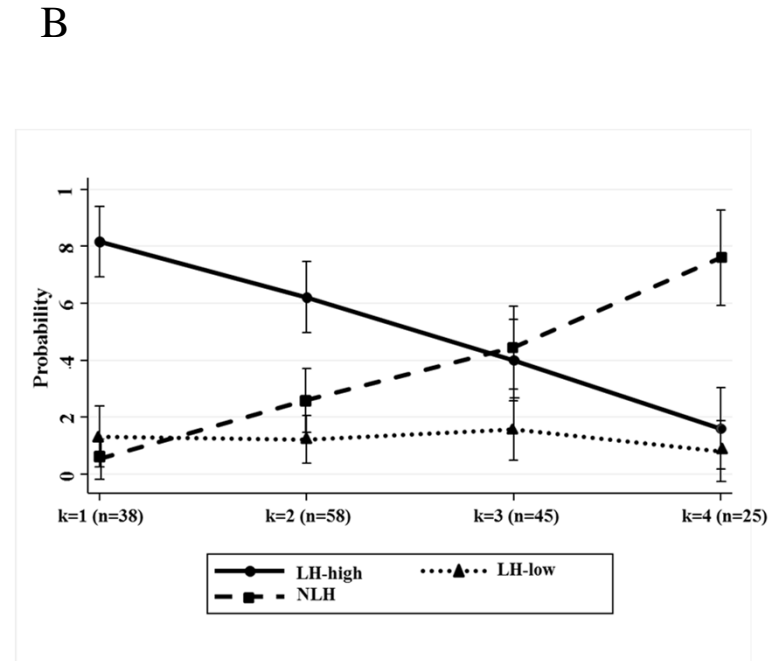


FIGURE 7.



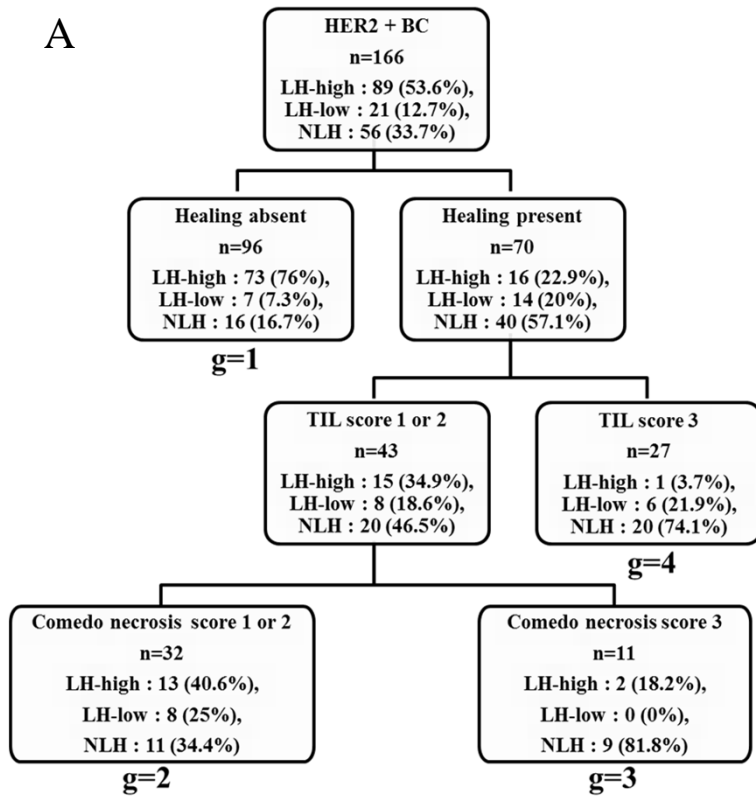


FIGURE 8.

